Physical Properties and Enzymatic Degradability of Copolymers of (*R*)-3-Hydroxybutyric and 6-Hydroxyhexanoic Acids

Hideki Abe and Yoshiharu Doi*

Polymer Chemistry Laboratory, The Institute of Physical and Chemical Research (RIKEN), Hirosawa, Wako-shi, Saitama 351-01, Japan

Hiromichi Aoki and Takashi Akehata

Department of Industrial Chemistry, Science University of Tokyo, 1-3, Kagurazaka, Shinjuku-ku, Tokyo 162, Japan

Yoji Hori and Akio Yamaguchi

Central Research Laboratory, Takasago International Corporation, 1-4-11, Nishiyahata, Hiratsuka-shi, Kanagawa 254, Japan

Received June 15, 1995; Revised Manuscript Received August 23, 1995®

ABSTRACT: Copolymers of (*R*)-3-hydroxybutyric acid ((*R*)-3HB) and 6-hydroxyhexanoic acid (6HH) with a wide range of compositions varying from 11 to 91 mol % 6HH were synthesized by the ring-opening polymerization of (*R*)-β-butyrolactone with ε-caprolactone at various feed ratios in the presence of 1-ethoxy-3-chlorotetrabutyldistannoxane as a catalyst. The structure and physical properties of P[(*R*)-3HB-*co*-6HH] were characterized by ^{1}H and ^{13}C NMR spectroscopy, X-ray diffraction, differential scanning calorimetry, and optical microscopy. The copolyesters were shown to have a random sequence distribution of (*R*)-3HB and 6HH monomeric units. The glass-transition temperature of P[(*R*)-3HB-*co*-6HH] decreased linearly from +4 to −67 °C as the 6HH composition was increased from 0 to 100 mol %. The melting temperature of P[(*R*)-3HB-*co*-6HH] samples decreased from 179 to 48 °C as the 6HH fraction was increased from 0 to 43 mol %. Then, the melting temperature of the copolyester increased from 36 to 60 °C with an increase in the 6HH fraction from 81 to 100 mol %. The degree of X-ray crystallinity of solvent-cast copolyester films decreased from 62 to 18% as the 6HH composition was increased from 0 to 43 mol %, and the copolyesters showed a P[(*R*)-3HB] crystal lattice. On the other hand, the X-ray crystallinities of copolymers with 6HH fractions of 81−100 mol % increased from 31 to 55% with the 6HH fraction, and those samples showed a P(6HH) crystal lattice. The P[(*R*)-3HB-*co*-6HH] samples with 53−70 mol % 6HH were amorphous polymers. Enzymatic degradations of P[(*R*)-3HB-*co*-6HH] films were carried out at 25 °C in 0.1 M potassium phosphate buffer (pH 7.4) in the presence of PHB depolymerase purified from *Alcaligenes faecalis* or of lipase from *Rhizopus delemar*. The rates of enzymatic degradation by PHB depolymerase of copolymer films ranging from 11 to 43 mol % 6HH were higher than that of bacterial P[(*R*)-3HB] film. The highest rate of enzymatic hydrolysis by PHB depolymerase was observed at 11 mol % 6HH. Little erosion was observed for the copolyester films ranging in 6HH fractions from 53 to 100 mol %. In contrast, the weight loss profile of P[(*R*)-3HB-*co*-6HH] films with a lipase showed a trend in the copolymer composition opposite to that of a PHB depolymerase. The highest rate of enzymatic hydrolysis by lipase was observed at 91 mol % 6HH. HPLC analysis of the water-soluble products liberated during the enzymatic degradation of copolymer films showed a mixture of monomers, dimers, and trimer of (*R*)-3HB and 6HH units. A model for the enzymatic hydrolysis of the polyester chain by PHB depolymerase was proposed on the basis of the results.

Introduction

An optically active poly[(*R*)-3-hydroxybutyrate] (P[(*R*)-3HB]) of pure isotactic structure is synthesized by a variety of bacteria as an intracellular storage material of carbon and energy.[1−3] Recently, many bacteria have been found to produce copolymers of (*R*)-3-hydroxyalkanoate units with carbon chains ranging from 4 to 14 carbon atoms.[3,4] In addition, several bacteria have been found to accumulate copolyesters containing hydroxyalkanoate monomeric units without side chains such as 3-hydroxypropionate (3HP),[5−7] 4-hydroxybutyrate (4HB),[8,9] and 5-hydroxyvalerate (5HV)[10] units. At present about 80 different monomeric units as constituents of bacterial poly(hydroxyalkanoates) (PHA) have been found.[4] These microbial polyesters are biodegradable and biocompatible thermoplastics, and the physical properties can be regulated by copolymerization,[11−13] blending,[14] processing,[15−17] cross-linking,[18] and introducing the functional groups.[19,20] The microbial polyesters have attracted industrial attention as an environmentally degradable material for a wide range of agricultural, marine, and medical applications.[1]

A remarkable characteristic of PHA is its biodegradability in the environment. Aerobic and anaerobic PHA-degrading bacteria and fungi have been isolated from various environments.[21−29] The microorganisms excrete extracellular PHB depolymerases to degrade environmental PHA and utilize the decomposed compounds as nutrients. The extracellular PHB depolymerases have been purified from some microorganisms such as *Pseudomonas lemoignei*,[30] *Pseudomonas pickettii*,[28] *Pseudomonas fluorescens*,[27] *Alcaligenes faecalis*,[23] *Comamonas testosteroni*,[29] and *Penicillium pinophilun*.[31]

Recently, Kumagai *et al.*[32] reported that the rate of enzymatic hydrolysis of P[(*R*)-3HB] film by the PHB depolymerase from *A. faecalis* increased with a decrease in the crystallinity. Mukai *et al.*[33] have investigated the substrate specificities of microbial PHB depolymerases on the enzymatic hydrolysis of various poly(hydroxyalkanoates). The PHB depolymerases hydrolyzed the

* To whom correspondence should be addressed.
® Abstract published in *Advance ACS Abstracts,* October 15, 1995.

0024-9297/95/2228-7630$09.00/0 © 1995 American Chemical Society

films of P[(R)-3HB], poly(3-hydroxypropionate) (P(3HP)), and poly(4-hydroxybutyrate) (P(4HB)), while the poly(5-hydroxyvalerate) (P(5HV)) and poly(6-hydroxyhexanoate) (P(6HH)) films were not eroded by the PHB depolymerases. The rates of enzymatic erosion of PHA films decreased in the following order: P[(R)-3HB] = P(3HP) > P(4HB) ≫ P(5HV) = P(6HH) = 0. These results suggest that the enzymatic degradability of PHA film with PHB depolymerases is regulated by both the chemical and solid-state structures of polyester. In fact, the rates of enzymatic degradation of copolyester films of poly[(R)-3-hydroxybutyrate-*co*-(R)-3-hydroxyvalerate] (P[(R)-3HB-*co*-(R)-3HV]),[36] poly[(R)-3-hydroxybutyrate-*co*-(R)-3-hydroxyhexanoate] (P[(R)-3HB-*co*-(R)-3HH]),[34] P[(R)-3HB-*co*-3HP],[7] and P[(R)-3HB-*co*-4HB][9,36] were strongly dependent on the copolymer composition. These results prompt us to investigate the physical properties and enzymatic degradability of the copolymers of (R)-3HB and 6HH units with a wide range of compositions.

It has been found that chemosynthetic PHA such as P(3HP) and P(6HH) are hydrolyzed by microbial lipases.[35] Mukai *et al.*[33] studied the enzymatic degradability of 5 different samples of microbial and chemosynthetic PHA with 16 different microbial lipases and reported the substrate specificities of lipases on the hydrolysis of PHA. The number of lipases capable of hydrolyzing PHA films decreased in the following order: P(3HP) > P(4HB) > P(5HV) > P(6HH). However, no lipase eroded bacterial P[(R)-3HB] film. The copolyester of (R)-3HB and 6HH units is an interesting sample for the study of the enzymatic degradabilities by PHB depolymerase and by lipase.

In this paper, we prepared the copolymers of (R)-3-hydroxybutyrate ((R)-3HB)) and 6-hydroxyhexanoate (6HH) by the ring-opening polymerization of (R)-β-butyrolactone with ε-caprolactone at various feed ratios in the presence of distannoxane as a catalyst.[37] The structure, thermal properties, and crystallization behavior of the copolymer were investigated by means of nuclear magnetic resonance (NMR), differential scanning calorimetry (DSC), X-ray diffraction, and optical microscopy. The enzymatic degradabilities of copolymer films were studied in the presence of PHB depolymerase from *A. faecalis* and of lipase from *Rhizopus delemar*. In addition, the water-soluble products during the enzymatic degradation of copolymer films were characterized by HPLC analysis.

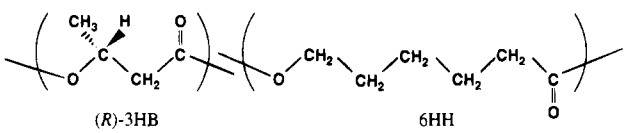

(R)-3HB 6HH

Experimental Section

Materials. 1-Ethoxy-3-chlorotetrabutyldistannoxane catalyst was prepared according to Okawara and Wada,[38] and the synthesis procedures were reported in our previous paper.[39] (R)-β-Butyrolactone[40] (ee 92%) ((R)-β-BL) was dried by CaH_2 and distilled under reduced pressure. The enantiomeric excess of (R)-β-BL was determined to be 92% by HPLC analysis. Bacterial poly[(R)-3-hydroxybutyrate] (P[(R)-3HB]) (M_n = 281 000, M_w/M_n = 2.3) was produced from butyric acid by *Alcaligenes eutrophus*.[41] Poly(6-hydroxyhexanoate) (P(6HH)) homopolymer was prepared by the ring-opening polymerization of ε-caprolactone (ε-CL) in the presence of methylaluminoxane (MAO). ε-CL (from Tokyo Kasei Kogyo Co., Tokyo) was dried on CaH_2 and distilled under nitrogen before use. The polymerization of ε-CL was carried out in toluene at 60 °C for 7 days. The number-average molecular weight and polydispersity of P(6HH) were M_n = 59 000 and M_w/M_n = 1.5, respectively.

Synthesis of P[(R)-3HB-*co*-6HH] Samples. Copolymers of (R)-3HB and 6HH were synthesized by the ring-opening polymerization of (R)-β-BL with ε-CL in the presence of 1-ethoxy-3-chlorotetrabutyldistannoxane as a catalyst. The copolymerization of β-butyrolactone and ε-CL with 1-ethoxy-3-chlorotetrabutyldistannoxane was carried out in the absence of solvent at 100 °C for 4 h under an argon atmosphere. The produced copolymer was dissolved in chloroform and precipitated in a mixture of diethyl ether and hexane (1/3). The precipitate was dried in vacuo at room temperature.

Preparation of Copolymer Films. Copolymer films (0.1 mm thickness) were prepared by solvent-casting techniques from chloroform solutions of P[(R)-3HB-*co*-6HH] using glass Petri dishes as casting surfaces. The films were aged at least 3 weeks at room temperature to reach equilibrium crystallinity prior to analysis. The amorphous polymers (53−70 mol % 6HH) were coated from a chloroform solution of polymer as a film of 0.1 mm thickness on a Teflon sheet and used for analysis.

Enzymatic Degradation. The extracellular PHB depolymerase from *A. faecalis* T1 was purified to electrophoretic homogeneity by the methods of Shirakura *et al.*[42] The lipase from *R. delemar* was purchased from Seikagaku Kogyo (Tokyo) and used without further purification. The enzymatic degradations of copolymer films were carried out at 25 ± 0.1 °C in 0.1 M potassium phosphate buffer (pH 7.4). The copolymer films (initial weights 14 mg, initial film dimensions: 10 × 10 × 0.1 mm) were placed in small bottles containing 1.0 mL of buffer. The reaction was started by the addition of 10 μL of an aqueous solution of PHB depolymerase (1.0 μg) or lipase (190 μg). For the weight loss measurement, the reaction solution was incubated with shaking, and the sample films were removed after reaction for a period of time, washed with distilled water, and dried to constant weight in vacuo before analysis. The water-soluble products after enzymatic degradation of copolymer films were examined by HPLC analysis of the reaction solution.

Analytical Procedures. All molecular weight data were obtained by gel-permeation chromatography at 40 °C, using a Shimadzu 6A GPC system and a 6A refractive index detector with Shodex K-80M and K-802 columns. Chloroform was used as eluent with a flow rate of 0.8 mL/min, and sample concentrations of 1.0 mg/mL were applied. The number-average and weight-average molecular weights (M_n and M_w) were calculated by using a Shimadzu Chromatopac C-R4A equipped with a GPC program. A molecular weight calibration curve of all polymer samples was obtained with polystyrene standards of low polydispersities.

The ^1H and ^{13}C NMR analyses of P[(R)-3HB-*co*-6HH] copolymers were carried out on a JEOL Alpha-400 spectrometer. The 400-MHz ^1H NMR spectra were recorded at 23 °C in a $CDCl_3$ solution of polymer (5 mg/mL) with a 5.5 μs pulse width (45° pulse angle), a 5 s pulse repetition, 8000 Hz spectral width, and 16K data points. The 100 MHz ^{13}C NMR spectra were recorded at 23 °C in a $CDCl_3$ solution of polymer (20 mg/mL) with a 5.5 μs pulse width (45° pulse angle), 5 s pulse repetition, a 25 000 Hz spectral width, 64K data points, and 13 000 accumulations.

DSC data of P[(R)-3HB-*co*-6HH] copolymers were recorded in the temperature range −150 to +200 °C on a Shimadzu DSC-50 equipped with a cooling accessory under a nitrogen flow of 30 mL/min. Samples of 10 mg were encapsulated in aluminum pans and heated from 0 to 200 °C at a rate of 10 °C/min (first scan). The peak melting temperature (T_m) and enthalpy of fusion (ΔH_m) were determined from the DSC endotherms. For measurement of the glass-transition temperature (T_g), the samples were maintained at 200 °C for 1 min and then rapidly quenched at −150 °C. They were then reheated from −150 to +200 °C at a heating rate of 20 °C/min (second scan). The T_g was taken as the midpoint of the heat capacity change.

The copolymer spherulitic morphologies were observed with a Nikon optical microscope equipped with crossed polarizers and a Linkham hot stage. The solvent-cast copolymer films

(2 mg) were first heated on a hot stage from room temperature to 200 °C at a rate of 30 °C/min. Samples were maintained at 200 °C for 30 s, and then the temperature was rapidly lowered to a given crystallization temperature (T_c) of 60−120 °C. The samples were crystallized isothermally at a given T_c to monitor the growth of the spherulites as a function of time. The radial growth rate of spherulites was calculated as the slope of the line obtained by plotting the spherulite radius against time with more than ten data points. For each crystallization measurement, the radial growth rates of the three different spherulites were recorded under the same conditions, and the spherulitic growth rates were averaged. During the thermal treatment, the copolymer films were kept under nitrogen flow in order to limit the degradation of the polymer. In order to minimize the risk of thermal degradation of copolymer, individual samples were used for each crystallization measurement.

The X-ray diffraction patterns of copolyester films were recorded at 27 °C on a Rigaku RAD-IIIB system using nickel-filtered Cu Kα radiation (λ = 0.154 nm; 40 kV; 30 mA) in the 2θ range 6−40° at a scan speed of 2.0°/min. Degrees of crystallinity (X_c) of the copolymer were calculated from diffracted intensity data according to Vonk's method.[43]

The surfaces of copolymer films were observed with a scanning electron microscope (JEOL JSM-5300) after gold coating of the films using an ion coater.

The water-soluble products of enzymatic degradation of copolymer films were analyzed by using a Shimadzu LC-9A HPLC system with a gradient controller and a SPD-10A UV spectrophotometric detector. A stainless steel column (250 × 4 mm) containing LiChrospher RP-8 (5 μm) was used at 40 °C. Sample solutions after the enzymatic degradation were acidified to pH 2.5 with HCl solution, and 50 μL solutions were injected. The column was eluted with a linear gradient of distilled water (pH 2.5, adjusted by the addition of HCl solution) to acetonitrile over 40 min with a flow rate of 1.0 mL/min. The monomer and oligomers of 3-hydroxybutyric acid and 6-hydroxyhexanoic acid were detected spectrophotometrically at a wavelength of 210 nm. The degradation products were fractionated by HPLC. Each product was collected from the HPLC eluate, and the solvent was evaporated and then used for ^{1}H NMR analysis. The 400 MHz ^{1}H NMR spectra were recorded in D_2O: 3HB monomer (t_R = 6.3 min), δ 1.20 (d, 3H), 2.42 (m, 2H), 4.21 (m, 1H); 6HH monomer (t_R = 11.6 min), δ 1.36 (m, 2H), 1.52−1.64 (m, 4H), 2.34 (t, 2H), 3.59 (t, 2H); 3HB−3HB dimer (t_R = 13.4 min), δ 1.21 (d, 3H), 1.30 (d, 3H), 2.45−2.66 (m, 4H), 4.22 (m, 1H), 5.26 (m, 1H); 6HH-3HB dimer (t_R = 16.3 min), δ 1.26 (d, 3H), 1.34 (m, 2H), 1.51−1.65 (m, 4H), 2.36 (t, 2H), 2.43 (m, 2H), 3.59 (t, 2H), 5.20 (m, 1H); 6HH−6HH dimer (t_R = 18.8 min), δ 1.36 (m, 4H), 1.51−1.69 (m, 8H), 2.36 (m, 4H), 3.59 (t, 2H), 4.12 (t, 2H); 3HB−6HH−3HB trimer (t_R = 19.7 min), δ 1.22 (d, 3H), 1.28 (d, 3H), 1.37 (m, 2H), 1.58−1.68 (m, 4H), 2.37 (m, 2H), 2.47−2.60 (m, 4H), 4.14 (m, 2H), 4.23 (m, 1H), 5.22 (m, 1H).

Results and Discussion

Synthesis and Structure of P[(*R*)-3HB-*co*-6HH] Copolymers. Copolyesters of (*R*)-3HB and 6HH were synthesized by the ring-opening polymerization of (*R*)-β-butyrolactone ((*R*)-β-BL) with ε-caprolactone (ε-CL) at various feed ratios from 90/10 to 10/90 (mol/mol) in the presence of 1-ethoxy-3-chlorotetrabutyldistannoxane as a catalyst. The copolymerization was carried out at 100 °C for 4 h under an argon atmosphere. The compositions of the copolymers were determined by integration of the proton resonances of the (*R*)-3HB and 6HH monomeric units in the ^{1}H NMR spectra. Table 1 shows the mole ratios of (*R*)-β-BL and ε-CL monomers used for the copolymerization and composition, the number-average molecular weight (M_n), and polydispersities (M_w/M_n) of produced copolymers. All experiments produced high yields of copolymers with high molecular weights (M_n > 10^5) at different mole ratios of (*R*)-β-BL to ε-CL, and the compositions of copolymers produced were in good agreement with the monomer feed ratios.

Table 1. Compositions and Molecular Weights of P[(*R*)-3HB-*co*-6HH] Copolymers

sample no.	monomer feed ratio, mol % (*R*)-β-BL	ε-CL	yield, %	composition,[a] mol % (*R*)-3HB	6HH	molecular weight[b] $10^{-3}M_n$	M_w/M_n
1[c]				100	0	281	2.3
2[d]	90	10	89	89	11	117	1.8
3	80	20	96	78	22	124	1.8
4	70	30	91	69	31	127	1.8
5	60	40	92	57	43	127	1.8
6	50	50	93	47	63	121	1.9
7	40	60	89	35	65	118	1.8
8	30	70	97	30	70	116	1.7
9	20	80	98	19	81	190	1.7
10	10	90	95	9	91	166	1.7
11[e]	0	100		0	100	59	1.5

[a] Determined from ^{1}H NMR spectra. [b] Determined by GPC analysis. [c] Bacterial poly[(*R*)-3-hydroxybutyrate]. [d] Samples 2−10 were synthesized by polmerizations of a mixture of (*R*)-β-BL and ε-CL with distannoxane catalyst. [e] Poly(6-hydroxyhexanoate) was synthesized by ring-opening polymerization of ε-CL with Al-based catalyst.

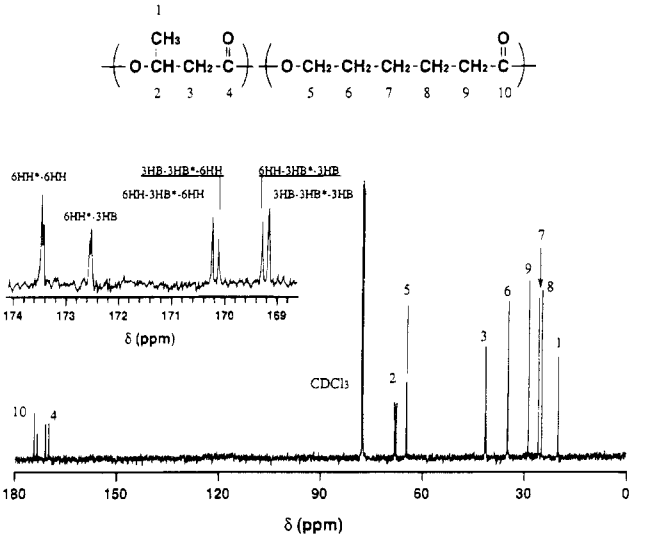

Figure 1. 100-MHz ^{13}C NMR spectrum of P[(*R*)-3HB-*co*-53 mol % 6HH] copolymer in $CDCl_3$ at 23 °C.

The sequence distributions of P[(*R*)-3HB-*co*-6HH] copolymers were determined from the 100 MHz ^{13}C NMR spectra. Figure 1 shows a ^{13}C NMR spectrum of the P[(*R*)-3HB-*co*-53 mol % 6HH] copolymer, together with the chemical shift assignment for each carbon resonance. The expanded carbonyl carbon resonances at 169.1−173.6 ppm (from Me_4Si) in Figure 1 were resolved into eight peaks due to triad sequences of (*R*)-3HB and 6HH units. The diad and triad fractions were calculated from the ratios of peak areas of carbonyl resonances. Table 2 lists the diad and triad fractions of copolymer samples, together with the ^{13}C chemical shift assignments. Hori *et al.*[40] reported that the distannoxane catalyst initiated ring-opening polymerization of lactones by breaking the bond between carbonyl carbon and the oxygen atoms of the lactone ring (acyl cleavage) and that the configuration of monomer was retained. The diad and triad sequence distribution data for two monomeric units were compared with Bernoullian statistics applicable to a statistically random copolymerization. In the Bernoullian model, the mole fraction F_{ij} of diad sequence ij can be expressed in terms of the mole fractions F_i and F_j of i and j units as

Table 2. Chemical Shifts and Relative Intensities of 13C Resonances in P[(R)-3HB-co-6HH] Copolymers

chemical shift, ppm	sequence	relative intensities[a] of sample 2	3	4	5	6	7	8	9	10
169.13	33*3	0.69	0.55	0.38	0.22	0.17	0.08	0.06	0.00	0.00
		(0.70)	(0.48)	(0.34)	(0.19)	(0.10)	(0.04)	(0.04)	(0.01)	(0.00)
169.24	63*3	0.12	0.13	0.16	0.14	0.13	0.10	0.07	0.00	0.00
		(0.09)	(0.13)	(0.14)	(0.13)	(0.12)	(0.08)	(0.06)	(0.03)	(0.01)
170.08	33*6	0.07	0.10	0.10	0.12	0.11	0.07	0.06	0.00	0.00
		(0.09)	(0.13)	(0.14)	(0.13)	(0.12)	(0.08)	(0.06)	(0.03)	(0.01)
170.21	63*6	0.02	0.03	0.08	0.13	0.13	0.14	0.12	0.09	0.05
		(0.01)	(0.04)	(0.07)	(0.11)	(0.13)	(0.15)	(0.15)	(0.12)	(0.07)
172.57	6*3	0.10	0.13	0.17	0.20	0.19	0.21	0.23	0.12	0.15
172.60		(0.10)	(0.17)	(0.21)	(0.25)	(0.25)	(0.23)	(0.21)	(0.15)	(0.08)
173.49	6*6	0.00	0.06	0.11	0.19	0.27	0.40	0.46	0.79	0.80
173.52		(0.01)	(0.05)	(0.10)	(0.19)	(0.28)	(0.42)	(0.49)	(0.66)	(0.83)

[a] The values in parentheses were calculated by Bernoullian statistics for the mole fraction of 6HH present in the copolymers. [b] See Table 1.

Table 3. Physical Properties of P[(*R*)-3HB-*co*-6HH] Copolymers

sample no.[a]	6HH fraction, mol %	T_g,[b] °C	T_m,[c] °C	ΔH_m,[d] J/g	X_c,[e] %
1	0	4	179	91	62 ± 5
2	11	−6	130	50	50 ± 5
3	22	−18	110	30	41 ± 5
4	31	−26	66	17	30 ± 5
5	43	−35	48	4	18 ± 5
6	53	−40	n.d.	0	0
7	65	−49	n.d.	0	0
8	70	−53	n.d.	0	0
9	81	−58	36	27	31 ± 5
10	91	n.d.[f]	47	55	36 ± 5
11	100	−67	60	60	55 ± 5

[a] See Table 1. [b] Glass-transition temperature; measured by DSC (second scan), from −150 to +200 °C at a rate of 20 °C/min. [c] Melting temperature; measured by DSC (first scan), from 0 to +200 °C at a rate of 10 °C/min. [d] Enthalpy of fusion; measured by DSC (first scan). [e] Degree of crystallinity; determined from X-ray diffraction patterns. [f] Not detected.

$F_{ij} = F_iF_j$ and the mole fraction F_{iji} of triad sequence *iji* as $F_{iji} = F_i^2F_j$. As shown in Table 2, the calculated diad and triad fractions are in good agreement with the observed values for all samples, indicating that the sequence distributions of (*R*)-3HB and 6HH units were statistically random.

Physical Properties of P[(*R*)-3HB-*co*-6HH] Samples. The T_g, T_m, and ΔH_m values of solution-cast copolymer films were determined from DSC thermograms. The results are given in Table 3, together with the values of microbial P[(*R*)-3HB] and poly(6-hydroxyhexanoate) films. The T_g values for P[(*R*)-3HB-*co*-6HH] copolymers decreased from +4 to −67 °C with an increase in the 6HH fraction from 0 to 100 mol %. The T_m values decreased from 177 to 48 °C as the 6HH fraction was increased from 0 to 43 mol %. Then, the T_m value increased from 36 to 60 °C with an increase in the 6HH fraction from 81 to 100 mol %. The fusion enthalpies of P[(*R*)-3HB-*co*-6HH] samples with 53 to 71 mol % 6HH were not detected due to amorphous polymers.

Figure 2 shows the X-ray diffraction patterns of solution-cast copolymer films with different 6HH fractions, together with the diffraction patterns for P[(*R*)-3HB] and P(6HH) homopolymers. For the copolyesters with compositions up to 43 mol % 6HH, only the crystalline form of the P[(*R*)-3HB] lattice was observed. In contrast, the P[(*R*)-3HB-*co*-6HH] copolymers with compositions of 81−100 mol % 6HH showed the P(6HH) crystal lattice. The degrees of X-ray crystallinity (X_c) of copolymer films are listed in Table 3. The X_c values

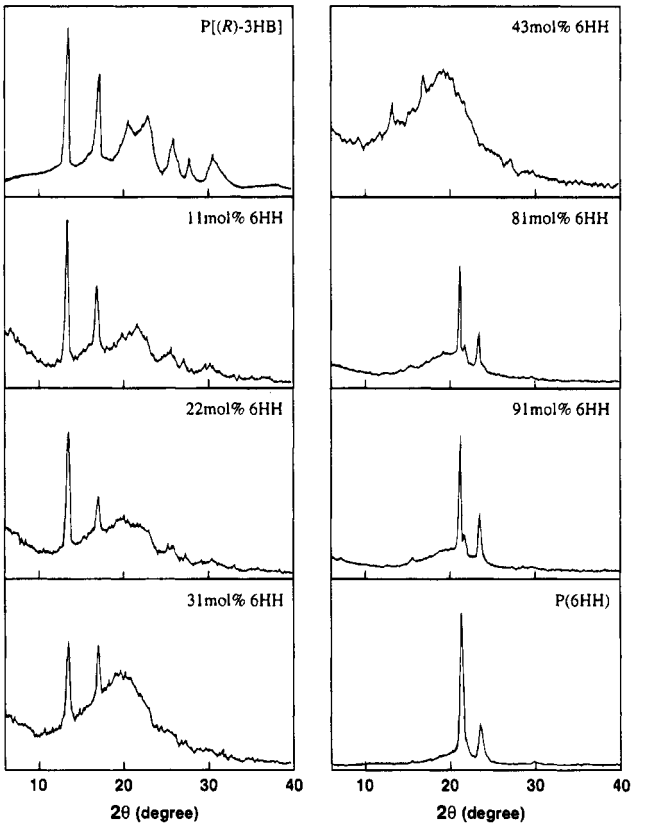

Figure 2. X-ray diffraction patterns of P[(*R*)-3HB-*co*-6HH] films with different 6HH fractions. Samples were prepared by the solution-cast method and aged for 3 weeks at room temperature.

of P[(*R*)-3HB-*co*-6HH] films decreased from 62 to 18% as the 6HH composition was increased from 0 to 43 mol %. The P[(*R*)-3HB-*co*-6HH] samples with 53 to 71 mol % 6HH were amorphous. Then, the X_c values increased from 31 to 55% with an increase in 6HH fraction from 81 to 100 mol %. The ΔH_m values showed a trend similar to the X_c values of copolymers.

The crystallization kinetics of P[(*R*)-3HB-*co*-6HH] were studied in the absence of nucleating agents. The spherulites of P[(*R*)-3HB-*co*-6HH] copolymers were observed with a polarized optical microscope. The samples were isothermally crystallized at a given temperature after melting at 200 °C for 30 s. Figure 3 shows typical optical micrographs of spherulites of the P[(*R*)-3HB-*co*-22 mol % 6HH] film crystallized at temperatures of 60, 70, and 90 °C. After crystallization, uniform spherulites were well-developed throughout the copolymer film. The spherulite radius increased linearly with time. The

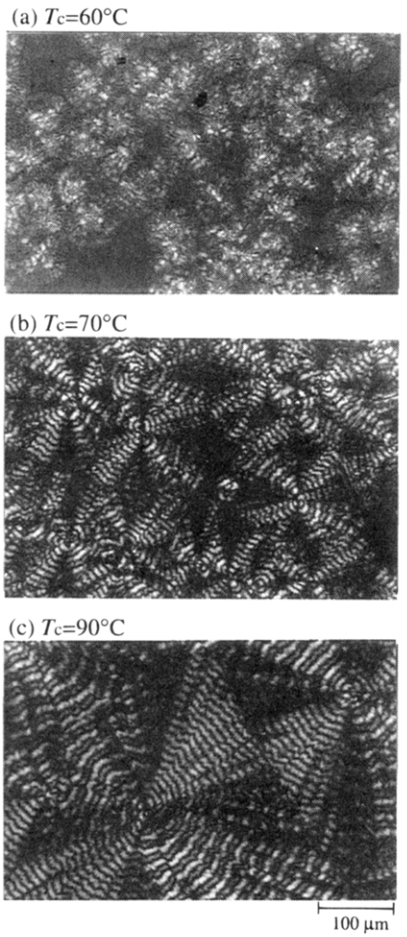

Figure 3. Optical micrographs of P[(*R*)-3HB-*co*-22 mol % 6HH] spherulites crystallized at 60 °C (a), at 70 °C (b), and at 90 °C (c).

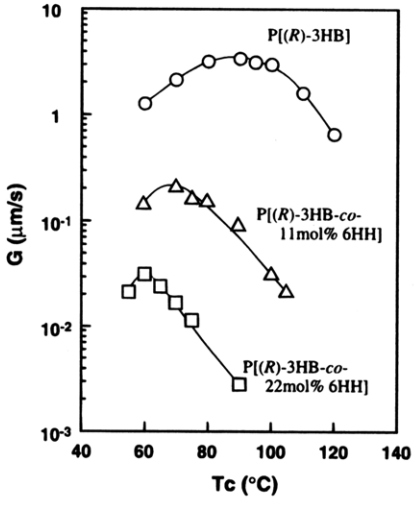

Figure 4. Radial growth rate (G) of spherulites as a function of crystallization temperature (T_c) for P[(*R*)-3HB] and P[(*R*)-3HB-*co*-6HH] with different 6HH fractions.

radial growth rate (G) of spherulites was calculated as the slope of the line obtained by plotting the spherulite radius against time. Figure 4 shows the rate of spherulite growth (G) of P[(*R*)-3HB-*co*-6HH] copolymers containing 0, 11, and 22 mol % 6HH unit at different crystallization temperatures. The rates of spherulite growth were dependent on both the 6HH composition and the crystallization temperature. A maximum value of 3.4 μm/s was observed around 90 °C for bacterial P[(*R*)-3HB]; however, as the 6HH component increased,

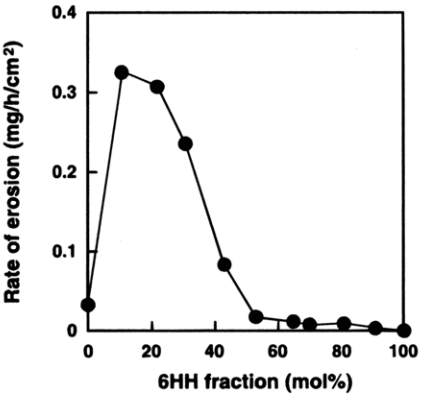

Figure 5. Effect of copolymer composition on the rate of enzymatic erosion of P[(*R*)-3HB-*co*-6HH] films in the aqueous solution of PHB depolymerase from *A. faecalis* at 25 °C and pH 7.4.

the spherulitic growth rates were remarkably reduced. In addition the crystallization curves were shifted toward lower temperatures. The radial growth rates of spherulites for the P[(*R*)-3HB-*co*-22 mol % 6HH] film were, in comparison, slower by 2 orders of magnitude than the rates determined for bacterial P[(*R*)-3HB], while the peak growth rate was observed near 65 °C. From this result we concluded that the randomly distributed 6HH units in the P[(*R*)-3HB-*co*-6HH] were responsible for the remarkable decrease in the rate of 3HB segments at the growth front of crystalline lamellae. The observed shift to a lower temperature for the spherulite growth curves of P[(*R*)-3HB-*co*-6HH] with respect to P[(*R*)-3HB], is attributed to the lower T_m values of the copolymers.

Enzymatic Degradation of Copolyester Films. The weight loss of P[(*R*)-3HB-*co*-6HH] films by PHB depolymerase from *A. faecalis* was measured at each 1 h for 5 h and increased proportionally with time. The values of weight loss of the sample films for 5 h were in the range 0−4 mg, depending on the copolymer composition. The rate of enzymatic erosion was determined from the slope of the line obtained by plotting the weight loss against time. Figure 5 shows the rates of enzymatic degradation at 25 °C of P[(*R*)-3HB-*co*-6HH] films by PHB depolymerase. No weight loss was observed for the P(6HH) homopolymer film by the PHB depolymerase. The rates of enzymatic degradation of P[(*R*)-3HB-*co*-6HH] films with 11−43 mol % 6HH were higher than that observed for the bacterial P[(*R*)-3HB] film. The highest rate of enzymatic degradation was observed with the copolymer film with 11 mol % 6HH, and the rate was about 10 times faster than that of bacterial P[(*R*)-3HB]. In contrast, very slow rates of enzymatic erosion were observed for the copolyesters with 53 to 91 mol % 6HH. In the absence of PHB depolymerase, P[(*R*)-3HB-*co*-6HH] films were not hydrolyzed for 24 h at 25 °C on 0.1 M potassium phosphate buffer.

Figure 6 shows the scanning electron micrographs (SEMs) of surfaces of copolymer films prior to and after enzymatic degradation. The surface of P[(*R*)-3HB-*co*-11 mol % 6HH] films after the enzymatic degradation for 3 h was apparently blemished by the function of depolymerase (Figure 6b), suggesting that the enzymatic degradation occurred on the surface of films. In contrast, the surface of the P[(*R*)-3HB-*co*-81 mol % 6HH] film with a little enzymatic erosion remained apparently unchanged after the film was incubated with PHB depolymerase for 3 h (Figure 6d).

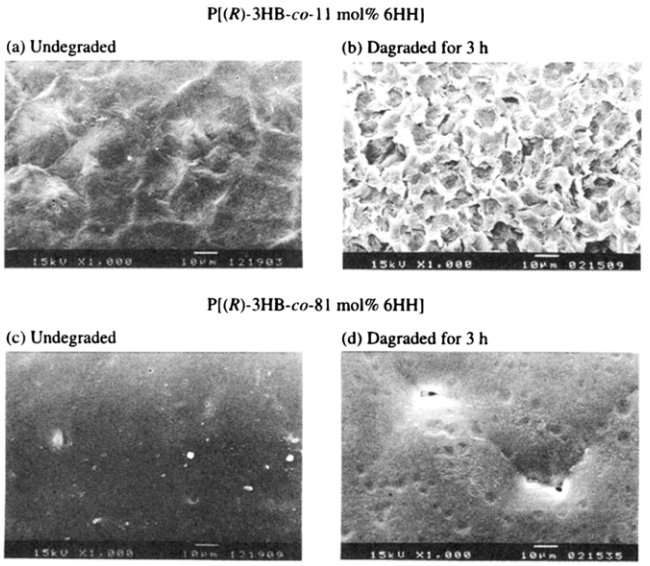

Figure 6. Scanning electron micrographs (SEMs) of surfaces of P[(*R*)-3HB-*co*-6HH] films before and after the enzymatic degradation of 3 h at 25 °C with PHB depolymerase from *A. faecalis*.

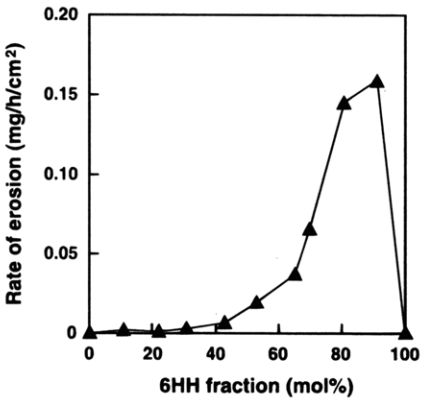

Figure 7. Effect of copolymer composition on the rate of enzymatic erosion of P[(*R*)-3HB-*co*-6HH] films in the aqueous solution of lipase from *R. delemar* at 25 °C and pH 7.4.

In a previous paper,[32] we reported that the rate of enzymatic degradation of bacterial P[(*R*)-3HB] film increased with a decrease in the crystallinity and that a PHB depolymerase from *A. faecalis* hydrolyzed predominantly the P[(*R*)-3HB] chains in the amorphous state on the surface of film. In addition, it was suggested that the rate of enzymatic degradation for the P[(*R*)-3HB] chains in the amorphous state was approximately 20 times higher than the rate for the P[(*R*)-3HB] chains in the crystalline state. The relative acceleration of enzymatic degradation for the P[(*R*)-3HB-*co*-11 mol % 6HH] film may be caused by the decrease in crystallinity. Although the crystallinities of films decreased with the 6HH fraction, the rates of enzymatic erosion on P[(*R*)-3HB-*co*-6HH] films with compositions of 11−43 mol % 6HH decreased markedly with an increase in the 6HH fraction. This result suggests that the rate of enzymatic degradation is regulated not only by the crystallinity of polymer but also by the chemical structure of monomeric units and the substrate specificity of PHB depolymerases.

The weight loss of P[(*R*)-3HB-*co*-6HH] films by a lipase from *R. delemar* was measured as a function of time for 19 h and increased proportionally with time. Figure 7 shows the rates of enzymatic degradation at 25 °C by the lipase. The film of P[(*R*)-3HB] homopolymer was not eroded by the lipase. It is of interest to note that the profiles of the degradation rates of P[(*R*)-3HB-*co*-6HH] films by both PHB depolymerase and lipase show symmetric curves against the copolymer composition. The rates of enzymatic degradation by lipase of P[(*R*)-3HB-*co*-6HH] films ranging in 6HH compositions from 53 to 91 mol % were faster than that of the P(6HH) homopolymer. The highest rate was observed on P[(*R*)-3HB-*co*-91 mol % 6HH], and very slow rates of enzymatic erosion were observed for copolymer films with 6HH compositions ranging from 0 to 43 mol %. In the absence of lipase, P[(*R*)-3HB-*co*-6HH] films were not hydrolyzed for 48 h at 25 °C on 0.1 M potassium phosphate buffer.

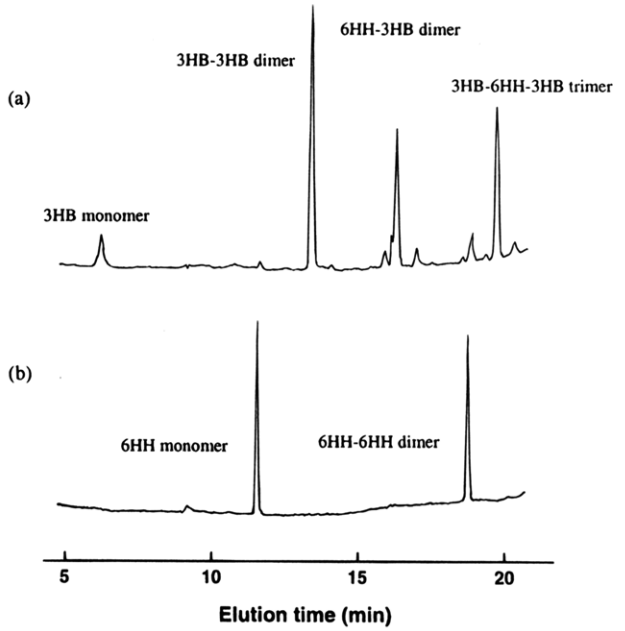

Figure 8. HPLC separations of water-soluble products after enzymatic degradation of (a) P[(*R*)-3HB-*co*-31 mol % 6HH] film with PHB depolymerase and (b) P[(*R*)-3HB-*co*-81 mol % 6HH] film with lipase.

Characterization of Water-Soluble Degradation Products. In a previous paper,[39] we reported that the enzymatic hydrolysis of bacterial P[(*R*)-3HB] film by PHB depolymerase produced a mixture of monomer and dimer of 3-hydroxybutyric acid as water-soluble products. In this study, we measured the composition of water-soluble products using HPLC analysis.

Figure 8 shows typical HPLC curves (at elution times of 0−20 min) of water-soluble products from P[(*R*)-3HB-*co*-6HH] films by PHB depolymerase (a) and by lipase (b). The component of each peak for the 3HB monomer, 6HH monomer, 3HB−3HB dimer, 6HH−3HB dimer, 6HH−6HH dimer, and 3HB−6HH−3HB trimer was identified by ^{1}H NMR analysis (see Experimental Section). The relative amounts of water-soluble products were determined from peak areas under HPLC curves.

The degradation of bacterial P[(*R*)-3HB] by PHB depolymerase yielded only two HPLC peaks, corresponding to the monomer and dimer of the (*R*)-3HB unit. In contrast, the HPLC curves of water-soluble products after the enzymatic degradation of P[(*R*)-3HB-*co*-6HH] films by PHB depolymerase showed four peaks at elution times from 0 to 20 min, corresponding to the 3HB monomer, 3HB−3HB dimer, 6HH−3HB dimer, and 3HB−6HH−3HB trimer. The peaks assignable to the 6HH monomer, 3HB−6HH dimer, and 6HH−6HH dimer as water-soluble products from PHB depoly-

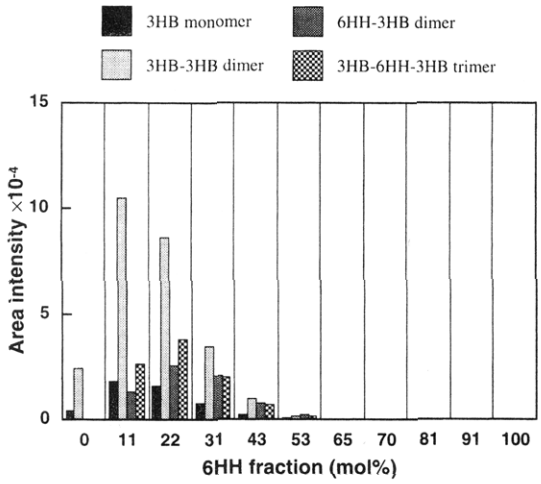

Figure 9. Distributions of water-soluble products after enzymatic degradation of P[(*R*)-3HB-*co*-6HH] films by PHB depolymerase for 5 h at 25 °C.

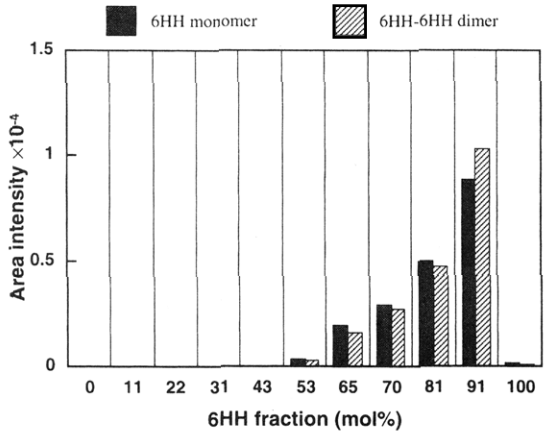

Figure 10. Distributions of water-soluble products after enzymatic degradation of P[(*R*)-3HB-*co*-6HH] films by lipase for 19 h at 25 °C.

merase action were not detected. This result suggests that the PHB depolymerase from *A. faecalis* is incapable of hydrolyzing the ester bonds of 6HH−3HB and 6HH−6HH sequences in dimers and oligomers. Figure 9 shows the relative amounts of water-soluble products after enzymatic degradation of P[(*R*)-3HB-*co*-6HH] films for 5 h at 25 °C by PHB depolymerase. The fractions corresponding to the 6HH−3HB dimer and 3HB−6HH−3HB trimer increased with an increase in the fraction of 6HH unit in copolymers.

Figure 10 shows the relative amounts of water-soluble products after enzymatic degradation of P[(*R*)-3HB-*co*-6HH] films for 19 h at 25 °C by lipase. The HPLC curves of the products showed only two peaks, arising from the 6HH monomer and 6HH−6HH dimer, and we could not detect the peaks from the monomer and dimers containing the 3HB unit. This result suggests that the lipase from *R. delemar* hydrolyzes only the ester bond of the 6HH−6HH sequence in a polymer chain.

Modeling of Enzymatic Cleavage of Ester Bonds by PHB Depolymerase. The enzymatic hydrolysis of P[(*R*)-3HB] by the PHB depolymerase from *A. faecalis* produced the 3HB dimer as the major product,[39] and only a small amount of 3HB monomer was produced, which suggests that the PHB depolymerase recognizes at least three monomeric units as substrate for the hydrolysis of ester bonds in a polymer chain. Kanesawa *et al.*[44] carried out NMR analysis of the

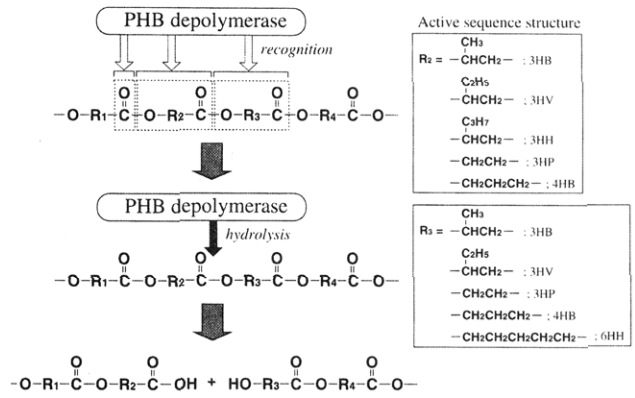

Figure 11. Schematic model for the enzymatic hydrolysis of an ester bond in various sequences by PHB depolymerase.

degradation products of poly[(*R*)-3-hydroxybutyrate-*co*-(*R*)-3-hydroxyvalerate] (P[(*R*)-3HB-*co*-(*R*)-3HV]) films by the PHB depolymerase from *A. faecalis*, and they reported that the 3HB monomer, 3HV monomer, 3HB−3HB dimer, 3HB−3HV dimer, 3HV−3HB dimer, and 3HV−3HV dimer were produced after enzymatic degradation of a P[(*R*)-3HB-*co*-41 mol % (*R*)-3HV] film for 5 h. However, the rate of enzymatic hydrolysis of the ester bond of the 3HV−3HV sequence was much slower than the rate of ester bond hydrolysis of the 3HB−3HB sequence. Recently, Doi *et al.*[34] have studied the enzymatic degradability of poly[(*R*)-3-hydroxybutyrate-*co*-(*R*)-3-hydroxyhexanoate] (P[(*R*)-3HB-*co*-(*R*)-3HH]) films by PHB depolymerase and characterized the water-soluble products by HPLC analysis. The water-soluble products from P[(*R*)-3HB-*co*-(*R*)-3HH] films were a mixture of the 3HB monomer, 3HB−3HB dimer, 3HB−3HH dimer, and 3HB−3HB−3HH trimer, while the 3HH monomer, 3HH−3HB dimer, and 3HH−3HH dimer were not detected. These results suggest that the PHB depolymerase is incapable of hydrolyzing the ester bonds of 3HB−3HH and 3HH−3HH sequences in dimers and oligomers. Mukai *et al.*[33] have investigated the enzymatic degradabilities of four PHA homopolymers of P(3HP), P(4HB), P(5HV), and P(6HH) by different PHB depolymerases. All PHB depolymerases used hydrolyzed the films of P(3HP) and P(4HB), while the P(5HV) and P(6HH) films were not eroded by PHB depolymerases, suggesting that PHB depolymerases are capable of cleaving the ester bonds of 3HP−3HP and 4HB−4HB sequences, while they are incapable of hydrolyzing the ester bonds of 5HV−5HV and 6HH−6HH sequences.

In this study, we found that the enzymatic degradation of P[(*R*)-3HB-*co*-6HH] films by PHB depolymerase gave the 3HB monomer, 3HB−3HB dimer, 6HH−3HB dimer, and 3HB−6HH−3HB trimer as water-soluble products. However, we could not detect the 6HH monomer, 6HH−6HH dimer, and 3HB−6HH dimer in the water-soluble products. It is of interest to note that the carboxyl-terminus of water-soluble products was always a 3HB unit, while the hydroxyl-terminus was either a 3HB or a 6HH unit. This result suggests that the PHB depolymerase from *A. faecalis* is capable of cleaving the ester bond of the 3HB−6HH sequence in a polymer chain, while incapable of hydrolyzing the ester bonds of 6HH−6HH and 6HH−3HB sequences.

These results led us to propose a model for enzymatic hydrolysis of ester linkages in a polymer (PHA) chain by PHB depolymerase (Figure 11). The primary degradation products of P[(*R*)-3HB] chains by PHB depoly-

merases were the monomer and dimer,[39] which may suggest preferential attack from the chain ends (*exo* attack). However, enzymatic hydrolysis of P[(*R*,*S*)-3HB] stereoisomers,[39,45] P[(*R*)-3HB-*co*-(*R*)-3HH],[34] and P[(*R*)-3HB-*co*-6HH] produced trimers and tetramers of monomeric units as degradation products with monomers and dimers. The results indicate that *endo* (random) cleavage of polyester chains by the depolymerase occurs together with *exo* cleavage, as suggested by the works of Hocking *et al.*[46,47] and Timmins *et al.*[48] In this model, we suggest that PHB depolymerase recognizes at least three monomeric units as substrate. The rate of enzymatic hydrolysis of an ester bond may be strongly dependent on the chemical structure of the second and third monomeric units in a polyester chain. PHB depolymerase may bind the substrate by interacting with the carbonyl group in the hydroxyl-terminated R_1 unit in order to assist the hydrolysis reaction of the second ester bond with the active site of depolymerase. The length of the main carbon chain of the second monomer R_2 unit may be limited to three or four carbon atoms because of a facile binding of substrate by PHB depolymerase. On the other hand, the chemical structure of the third monomer R_3 unit may affect the accessibility of the ester bond to the active site of PHB depolymerase. When the third monomeric unit has a sterically bulky side chain, PHB depolymerase may hardly attack the ester bond. Consequently, the hydrolysis rate of ester bonds by PHB depolymerase decreases as the side-chain length of a hydroxyalkanoate unit increases.

References and Notes

(1) Holmes, P. A. In *Developments in Crystalline Polymers—2*; Bassett, D. C., Ed.; Elsevier: London, 1988; p 1.
(2) Doi, Y. *Microbial Polyesters*; VCH Publishers: New York, 1990.
(3) Anderson, A. J.; Dawes, E. A. *Microbiol. Rev.* **1990**, *54*, 450.
(4) Steinbüchel, A.; Valentin, H. E. *FEMS Microbiol Lett.* **1995**, *128*, 219.
(5) Nakamura, S.; Kunioka, M.; Doi, Y. *Macromol. Rep.* **1991**, *A28*, 15.
(6) Hiramitsu, M.; Doi, Y. *Polymer* **1993**, *34*, 4782.
(7) Shimamura, E.; Scandola, M.; Doi, Y. *Macromolecules* **1994**, *27*, 4429.
(8) Doi, Y.; Kunioka, M.; Nakamura, Y.; Soga, K. *Macromolecules* **1988**, *21*, 2722.
(9) Nakamura, S.; Doi, Y.; Scandola, M. *Macromolecules* **1992**, *25*, 4237.
(10) Doi, Y.; Tamaki, A.; Kunioka, M.; Soga, K. *Makromol. Chem., Rapid Commun.* **1987**, *8*, 631.
(11) Marchessault, R. H.; Bluhm, T. L.; Deslandes, Y.; Hamer, G. K.; Orts, W. J.; Sundaarajan, P. R.; Taylor, M. G.; Bloembergen, S.; Holden, D. A. *Makromol. Chem., Macromol. Symp.* **1988**, *19*, 235.
(12) Inoue, Y.; Yoshie, N. *Prog. Polym. Sci.* **1992**, *17*, 571.
(13) Barham, P. J.; Barker, P.; Organ, S. J. *FEMS Microbiol. Rev.* **1992**, *103*, 189.
(14) Verhoogt, H.; Ramsay, B. A.; Favis, B. D. *Polymer* **1994**, *35*, 5155.
(15) Yasin, M.; Holland, S. J.; Tighe, B. J. *Biomaterials* **1990**, *11*, 206.
(16) De Koning, G. J. M.; Lemstra, P. J. *Polymer* **1993**, *34*, 4089.
(17) De Koning, G. J. M.; Scheeren, A. H. C.; Lemstra, P. J.; Peeters, M.; Reynaers, H. *Polymer* **1994**, *35*, 4598.
(18) De Koning, G. J. M.; Van Bilsen, H. H. M.; Lemstra, P. J.; Hazenberg, W.; Witholt, B.; Preusting, H.; Van der Galiën, J. G.; Schirmer, A.; Jendrossek, D. *Polymer* **1994**, *35*, 2090.
(19) Kim, Y. B.; Lenz, R. W.; Fuller, R. C. *Macromolecules* **1991**, *24*, 5356.
(20) Kim, Y. B.; Lenz, R. W.; Fuller, R. C. *Macromolecules* **1992**, *25*, 1852.
(21) Chowdhury, A. A. *Arch. Microbiol.* **1963**, *47*, 167.
(22) Delafield, F. P.; Doudoroff, M.; Pallerroni, N. J.; Lusty, C. J.; Contopoulos, R. *J. Bacteriol.* **1965**, *90*, 1455.
(23) Tanio, T.; Fukui, T.; Shirakura, Y.; Saito, T.; Tomita, K.; Kaiho, T.; Masamune, S. *Eur. J. Biochem.* **1982**, *124*, 71.
(24) Jansen, P. H.; Harfoot, C. G. *Arch. Microbiol.* **1990**, *154*, 253.
(25) Mergaert, J.; Anderson, C.; Wouters, A.; Swings, J.; Kersters, K. *FEMS Microbiol. Rev.* **1992**, *103*, 317.
(26) Jendrossek, D.; Knode, I.; Habibian, R. B.; Steinbüchel, A.; Schlegel, H. G. *J. Environ. Polym. Degrad.* **1993**, *1*, 53.
(27) Schirmer, A.; Jendrossek, D.; Schlegel, H. G. *Appl. Environ. Microbiol.* **1993**, *59*, 1220.
(28) Yamada, K.; Mukai, K.; Doi, Y. *Int. J. Biol. Macromol.* **1993**, *15*, 215.
(29) Mukai, K.; Yamada, K.; Doi, Y. *Polym. Degrad. Stab.* **1993**, *41*, 85.
(30) Lusty, C. J.; Doudoroff, M. *Proc. Natl. Acad. Sci. U.S.A.* **1966**, *56*, 960.
(31) Brucato, C. L.; Wong, S. S. *Arch. Biochem. Biophys.* **1991**, *290*, 497.
(32) Kumagai, Y.; Kanesawa, Y.; Doi, Y. *Makromol. Chem.* **1992**, *193*, 53.
(33) Mukai, K.; Doi, Y.; Sema, Y.; Tomita, K. *Biotechnol. Lett.* **1993**, *15*, 601.
(34) Doi, Y.; Kitamura, S.; Abe, H. *Macromolecules* **1995**, *28*, 4822.
(35) Tokiwa, Y.; Suzuki, T. *Nature* **1977**, *270*, 76.
(36) Doi, Y.; Kanesawa, Y.; Kunioka, M.; Saito, T. *Macromolecules* **1990**, *23*, 26.
(37) Hori, Y.; Takahashi, Y.; Yamaguchi, A.; Nishishita, T. *Macromolecules* **1993**, *26*, 4388.
(38) Okawara, R.; Wada, M. *J. Organomet. Chem.* **1963**, *1*, 81.
(39) Abe, H.; Matsubara, I.; Doi, Y.; Hori, Y.; Yamaguchi, A. *Macromolecules* **1994**, *27*, 6018.
(40) Hori, Y.; Suzuki, M.; Yamaguchi, A.; Nishishita, T. *Macromolecules* **1993**, *26*, 5533.
(41) Doi, Y.; Tamaki, A.; Kunioka, M.; Soga, K. *Appl. Microbiol. Biotechnol.* **1988**, *28*, 330.
(42) Shirakura, Y.; Fukui, T.; Saito, T.; Okamoto, Y.; Narikawa, T.; Koide, K.; Tomita, K.; Takemasa, T.; Masamune, S. *Biochim. Biophys. Acta* **1986**, *880*, 46.
(43) Vonk, C. G. *J. Appl. Crystallogr.* **1973**, *6*, 148.
(44) Kanesawa, Y.; Tanahashi, N.; Doi, Y.; Saito, T. *Polym. Degrad. Stab.* **1994**, *45*, 179.
(45) Abe, H.; Matsubara, I.; Doi, Y. *Macromolecules* **1995**, *28*, 844.
(46) Hocking, P. J.; Marchessault, R. H.; Timmins, M. R.; Scherer, T. M.; Lenz, R. W.; Fuller, R. C. *Macromol. Rapid Commun.* **1994**, *15*, 447.
(47) Hocking, P. J.; Timmins, M. R.; Scherer, T. M.; Fuller, R. C.; Lenz, R. W.; Marchessault, R. H. *J. Macromol. Sci., Pure Appl. Chem.* **1995**, *A32*, 889.
(48) Timmins, M. R.; Lenz, R. W.; Hocking, P. J.; Marchessault, R. H.; Fuller, R. C. *Macromol. Chem. Phys.*, submitted for publication.

MA950838K